

# Magnetic properties and Curie temperatures of disordered Heusler compounds: $\text{Co}_{1+x}\text{Fe}_{2-x}\text{Si}$

Julia Erika Fischer,<sup>1</sup> Julie Karel,<sup>1,\*</sup> Simone Fabbrici,<sup>2</sup> Peter Adler,<sup>1</sup>  
Siham Ouadi,<sup>1</sup> Gerhard H. Fecher,<sup>1</sup> Franca Albertini,<sup>2</sup> and Claudia Felser<sup>1</sup>

<sup>1</sup>*Max Planck Institute for Chemical Physics of Solids, D-01187 Dresden, Germany*

<sup>2</sup>*Institute of Materials for Electronics and Magnetism, I-43124 Parma, Italy*

(Dated: April 22, 2016)

The local atomic environments and magnetic properties were investigated for a series of  $\text{Co}_{1+x}\text{Fe}_{2-x}\text{Si}$  ( $0 \leq x \leq 1$ ) Heusler compounds. While the total magnetic moment in these compounds increases with the number of valence electrons, the highest Curie temperature ( $T_C$ ) in this series was found for  $\text{Co}_{1.5}\text{Fe}_{1.5}\text{Si}$ , with a  $T_C$  of 1069 K (24 K higher than the well known  $\text{Co}_2\text{FeSi}$ ). <sup>57</sup>Fe Mössbauer spectroscopy was used to characterize the local atomic order and to estimate the Co and Fe magnetic moments. Consideration of the local magnetic moments and the exchange integrals is necessary to understand the trend in  $T_C$ .

PACS numbers: 75.30.Cr, 76.80.+y, 75.50.Bb, 85.75.-d

## I. INTRODUCTION

$\text{Co}_2$ -based Heusler compounds belong to one of the most promising classes of materials for high performance spintronic devices because they have been predicted to be half-metallic ferromagnets (HMF)<sup>1–4</sup>. These materials exhibit complete spin polarization, arising from a band gap at the Fermi energy for the minority electrons and metallic-like behavior of majority carriers<sup>5–8</sup>. This high spin polarization has been recently demonstrated experimentally<sup>9</sup>. The compounds with high magnetic moments also exhibit high Curie temperatures, for example, well ordered  $\text{Co}_2\text{FeSi}$  has a magnetic moment of  $6 \mu_B$  and a  $T_C$  of 1040 K [10], making these materials important for applications. High Curie temperatures in HMF are desirable for stable spintronic devices because they reduce magnetic fluctuations at the working temperatures that are usually above room temperature.

Previous studies have shown that the total magnetic moment of  $\text{Co}_2$ -based half-metallic ferromagnetic Heusler compounds increases linearly over a large range of the number of valence electrons ( $N_{\text{VE}}$ ). This linear dependence is derived from the well-known Slater–Pauling rule<sup>8,11,12</sup>. Further, it was found that the Curie temperatures of these materials increase with increasing magnetic moment<sup>12,13</sup>, with a dependence that seems to be nearly linear over a wide range of magnetic moments (see Figure 1). In a simple spin-only molecular field approach,  $T_C$  should scale with the square of the spin ( $T_C \propto S(S+1)$ ). It was thus suggested that the linearity in  $m$ , which is proportional to  $S$ , is caused by modifications in the Heisenberg exchange coupling coefficients<sup>12</sup>. Figure 1 shows a plot of known Curie temperatures of  $\text{Co}_2$  based Heusler compounds. It is evident that most of the data points are outside of the 95% confidence bounds. The statistical significance for a linear model may thus not be very high. In fact, deviations from the linear trend have already been discussed in Reference [13], where it was shown theoretically that in par-

ticular compounds with 27 valence electrons exhibit significantly lower Curie temperatures resulting from a drastic change in the exchange coupling coefficients at this valence electron concentration. Based on the electronic structure calculations for compounds with more than 27 valence electrons, it was found that the exchange average only slightly increases, and the upward trend in the Curie temperatures is due to the large local moments. In other cases, the measured and calculated Curie temperatures and magnetic moments deviate from each other because of disorder in the investigated samples that is not accounted for in the theoretical approaches. It is further seen from Figure 1 that large deviations from an increasing trend are found in small regions around a selected magnetic moment where one actually may observe a decrease. Therefore, it is worth analyzing the behavior of the Curie temperatures in a small range of magnetic moments and investigating the influence of disorder on the  $T_C - m$  relation. The present work investigates Heusler compounds that are known to exhibit extremely high Curie temperatures<sup>10,14</sup>, namely  $\text{Co}_{1+x}\text{Fe}_{2-x}\text{Si}$ . The valence electron concentration varies by only one electron in this series where  $x$  is between 0 and 1; therefore, the magnetic moments vary also by just  $1 \mu_B$ .

## II. EXPERIMENTAL METHODS

Polycrystalline  $\text{Co}_{1+x}\text{Fe}_{2-x}\text{Si}$  samples with  $x = 0, 0.2, 0.4, 0.5, 0.6$ , and  $1.0$  were synthesized by arc melting. Stoichiometric amounts of the elements (purity of 99.999% or higher) were arc melted on a water cooled copper hearth under argon atmosphere. The ingots were remelted four times to improve the samples' homogeneity. They were put in a welded tantalum tube, and annealing was carried out in a sealed quartz ampoule, followed by rapid quenching in a mixture of ice and water.  $\text{Co}_2\text{FeSi}$  was annealed at 1300 K for 21 days,  $\text{CoFe}_2\text{Si}$  was annealed at 1073 K for 4 days, and the samples with inter-

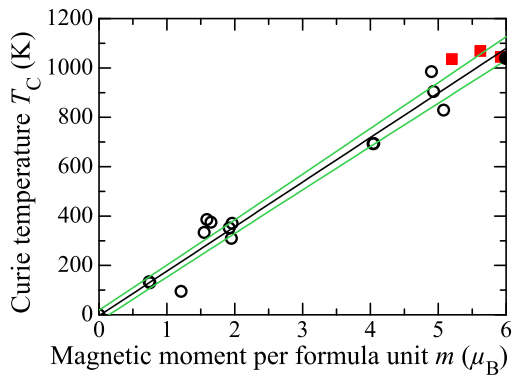


FIG. 1. (Color online) Dependency of the  $T_C$  on the magnetic moment for  $\text{Co}_2$ -based Heusler compounds. Data for open circles are collected from Reference [15]. The closed circle data point at  $m = 6 \mu_B$  is taken from Reference [10]. Closed squares are from the measurements reported in this work. The lines result from a fit of the cited data to a linear model and give the expectation in the 95% confidence interval.

mediate stoichiometry were annealed at 1000 K for 7 days to the homogeneity and crystalline structures<sup>15–17</sup>.

The composition and phase homogeneity of the samples were verified by wavelength dispersive X-ray spectroscopy (WDS) using a Cameca SX 100 electron microprobe. Wavelength dispersive X-ray spectroscopy revealed that obtained and nominal target compositions are in good agreement within the experimental uncertainty (see Table I). Therefore, the compounds will be described in the following by their nominal compositions.

The structure was determined and the phase homogeneity further verified by powder X-ray diffraction using an image plate Huber G670 Guinier camera with a  $\text{Ge}(111)$  monochromator and  $\text{Co K}_\alpha$  radiation. To collect the data, the samples were evenly distributed on Mylar foil and a pattern in the range of  $2\theta = 10^\circ - 100^\circ$  was recorded at room temperature. For determination of the lattice parameters, the silicon standard reference material® 640c was added. Indexing and refinement of the lattice parameter was done with the programs WIN XPOW<sup>18</sup> and PowderCell<sup>19</sup>.

Magnetostructural investigations were performed at room temperature using  $^{57}\text{Fe}$  Mössbauer spectroscopy on a standard WissEl spectrometer operated in the constant acceleration mode and equipped with a  $^{57}\text{Co}/\text{Rh}$  source. The powdered samples containing approximately  $10 \text{ mg}/\text{cm}^2$  of Fe were diluted with boron nitride to ensure a homogeneous distribution. Acrylic glass sample containers were used. All isomer shifts are given relative to  $\alpha$ -iron. The data were evaluated with the MossWinn<sup>20</sup> program using the thin absorber approximation. Hyperfine field distributions were derived using the Hesse-Rübartsch method implemented in MossWinn.

The magnetization and hysteresis were measured with a SQUID magnetometer (Quantum Design; MPMS 3 or MPMS XL7). The measurements were carried out at

1.8 K in induction fields in the range of -5 to +5 T. Temperature dependent AC susceptibility measurements were performed using thermomagnetic analysis (TMA) in order to determine the Curie temperature of the samples. Data were collected in a home-built susceptometer with a working temperature range from room temperature to 1373 K. An alternating magnetic induction field of 0.4 mT was applied. The instrumental precision is  $\pm 2 \text{ K}$  derived from the sensor's accuracy and calibration with an iron standard sample. A description of the TMA principle is found in Reference [21].

### III. RESULTS

#### A. Structural Analysis

Figure 2 shows the two different structure types that occur for ordered Heusler compounds generally. The two structure types are the regular  $L2_1$  type ( $\text{Cu}_2\text{MnAl}$ , cF16,  $Fm\bar{3}m$ , 225) and the inverse X type ( $\text{Li}_2\text{AgSb}$ , cF16,  $F\bar{4}3m$ , 216). In the  $\text{Co}_{1+x}\text{Fe}_{2-x}\text{Si}$  series, the general atoms assigned in Figure 2 by X, Y, and Z correspond to Co, Fe, and Si, respectively.

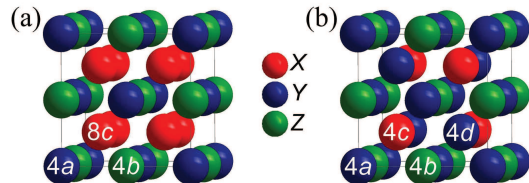


FIG. 2. (Color online) Crystal structures of  $\text{Co}_2\text{FeSi}$  and  $\text{Fe}_2\text{CoSi}$ .

Shown are: (a) the regular Heusler  $L2_1$  structure (space group 225) and (b) the inverse X structure (space group 216). The atoms are labeled by the corresponding Wyckoff positions.

Selected results from powder XRD are shown in Figure 3. The diffraction patterns were indexed using a face centered cubic cell (Figure 3). The lattice constant is  $a = 5.64 \text{ \AA}$  for all samples. This corresponds to the lattice parameters found in other works<sup>10,14,22,23</sup>. Major changes of the lattice parameters are not expected within the composition of the series because the radii of Co and Fe differ by about  $0.01 \text{ \AA}$  only<sup>24</sup>.

In the X-ray diffraction pattern of  $\text{Co}_2\text{FeSi}$  traces of a minority phase (whose estimated weight fraction is less than 1%) are deduced by the presence of extremely small peaks around  $2\theta = 51^\circ$  and  $2\theta = 9^\circ$ . The investigations discussed below in Sections III B and III C will show that these minor impurities do not affect the magnetic properties of the sample. The X-ray diffraction patterns of the other samples do not indicate secondary phases.

An analysis of the intensities of the diffraction peaks shows that the theoretical patterns of the corresponding ordered structures (Figure 3, right) exhibit different intensity ratios than the experimental patterns. Corre-

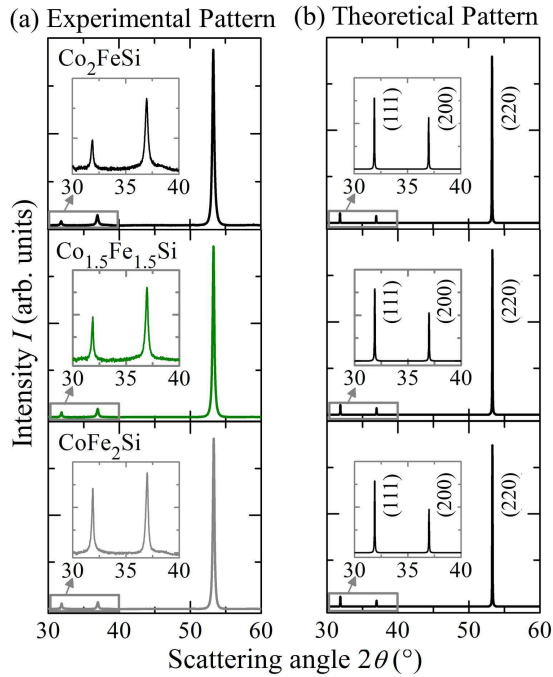


FIG. 3. (Color online) Powder XRD of selected  $\text{Co}_{2-x}\text{Fe}_{1+x}\text{Si}$  samples

Representative (a) experimental and (b) theoretical X-ray diffraction patterns of  $\text{Co}_2\text{FeSi}$ ,  $\text{Co}_{1.5}\text{Fe}_{1.5}\text{Si}$  and  $\text{CoFe}_2\text{Si}$ . The theoretical patterns were calculated for the well ordered structures with Co replacing Fe on the 4d position of the X type structure.

sponding values are given in Table I. This result demonstrates that disorder is present in the samples. A detailed Rietveld analysis reveals that the  $\text{Co}_2\text{FeSi}$  sample exhibits a large degree of Fe-Si anti site disorder and is composed of 80%  $L2_1$  and 20%  $B2$  type phases. The type of disorder in  $\text{Fe}_2\text{CoSi}$  is not easily distinguished; it is likely composed of about 30 to 35% of a  $B2$  type phase with the remaining phase adopting either an  $L2_1$  type or X type structure. A determination of the type of disorder is even further complicated in the mixed compounds due to the relatively similar scattering parameters of Fe and Co. More details of the disordered structures and the local environments of the Fe atoms will be discussed in Section III C, which presents results from  $^{57}\text{Fe}$  Mössbauer spectroscopy.

### B. Magnetic Properties

The field dependency of the magnetization was studied at 1.8 K, and the behavior is typical of soft magnetic materials. The saturation magnetization per formula unit has values between 5 and  $6\mu_B$ . The moment of  $\text{Co}_2\text{FeSi}$  is  $5.92\mu_B$ , which is in good agreement with previous work ( $5.91\mu_B$  at 10 K [23] and  $5.97\mu_B$  at 5 K [10]). The Slater–Pauling rule describes the dependence of the mag-

netic moment on the valence electron concentration. For ordered, half-metallic ferromagnetic Heusler compounds this dependence is given by<sup>12</sup>:

$$m = N_v - 24. \quad (1)$$

The experimentally determined values follow this equation only roughly (Figure 8 (a)). The slightly higher values found for  $m$  in the Fe rich members of this series are not unusual. Similar deviations from the theoretical values have been reported previously for Heusler compounds<sup>12</sup>.

The Curie temperatures were determined by measuring the AC susceptibility. The results are shown in Figure 4. In this experiment, the temperature dependence of the initial AC susceptibility  $\chi_{AC}$  provides the magnetic critical temperatures of the samples. Since the recorded AC susceptibility is influenced by many extrinsic features, such as microstructure, grain texture and lattice defects, the measurements shown in Figure 4 were normalized to the maximum values. The shallow dip that is observed in some measurements below the Curie temperature is due to the fact that the samples were not measured at saturation but in a field of only 0.4 mT.

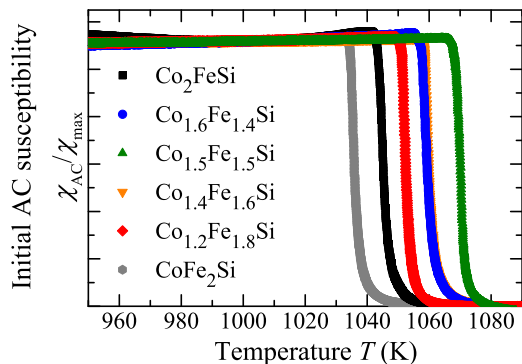


FIG. 4. (Color online) Heating curves of the AC susceptibility measurements near the Curie point.

The Curie temperatures are determined from the inflection point of the registered curves. The width of the transition depends on the applied magnetic field and sample homogeneity. The full width at half maximum of the first derivative of the curve as well as the instrumental precision were taken into account for determining the accuracy of the obtained Curie temperatures. Hence, the  $T_C$  of  $\text{Co}_2\text{FeSi}$  is 1045 K with an uncertainty of 0.4%. This value compares well with the inflection point of the magnetization versus temperature measurements reported in Reference [25].

The  $T_C$  of the series changes with iron content, where it reaches a maximum for  $x = 1/2$  (see Figure 8 (b)). The maximum Curie temperature of 1069 K found for  $\text{Co}_{1.5}\text{Fe}_{1.5}\text{Si}$  is 24 K higher than the value derived for  $\text{Co}_2\text{FeSi}$ .

TABLE I. Results of the phase analysis of the alloys  $\text{Co}_{1+x}\text{Fe}_{2-x}\text{Si}$  and representative intensity ratios derived from the experimental and theoretical X-ray diffraction patterns for  $\text{Co}_2\text{FeSi}$ ,  $\text{CoFe}_2\text{Si}$  and  $\text{Co}_{1.5}\text{Fe}_{1.5}\text{Si}$  from the patterns shown in Figure 3. The relative error of the composition is 0.30% for Si and 0.45% for Co and Fe for the values derived from WDS, which leads to the same uncertainty in the number of valence electrons.

$x$	$N_v$	target composition			WDS composition			experimental XRD			theoretical XRD		
		Co	Fe	Si	Co	Fe	Si	$I_{111}/I_{200}$	$I_{111}/I_{220}$	$I_{200}/I_{220}$	$I_{111}/I_{200}$	$I_{111}/I_{220}$	$I_{200}/I_{220}$
0	29	1.00	2.00	1.00	1.01	2.00	0.99	0.53	0.02	0.03	1.64	0.06	0.04
0.2	29.2	1.20	1.80	1.00	1.20	1.81	0.99	-	-	-	-	-	-
0.4	29.4	1.40	1.60	1.00	1.40	1.61	0.99	-	-	-	-	-	-
0.5	29.5	1.50	1.50	1.00	1.51	1.51	0.98	0.50	0.02	0.04	1.49	0.06	0.04
0.6	29.6	1.60	1.40	1.00	1.60	1.41	0.99	-	-	-	-	-	-
1	30	2.00	1.00	1.00	1.99	1.01	1.00	0.25	0.01	0.05	1.37	0.06	0.04

### C. $^{57}\text{Fe}$ Mössbauer Spectroscopy

$^{57}\text{Fe}$  Mössbauer spectroscopy is well suited to unravel the atomic order in  $\text{Co}_{1+x}\text{Fe}_{2-x}\text{Si}$  Heusler alloys<sup>16</sup>. The Mössbauer spectra of the compounds are composed of hyperfine sextets as expected for magnetically ordered phases (representative spectra are shown in Figure 5). All spectra exhibit some line broadening in addition to the linewidth of the  $\alpha\text{-Fe}$  standard and also some asymmetry. Therefore, the spectra were evaluated with distributions of hyperfine fields  $B_{\text{hf}}$  rather than with single sextets of Lorentzian shape. The results of the data analysis are summarized in Table II, where  $IS$  corresponds to the isomer shifts and  $\langle B_{\text{hf}} \rangle$  to the average hyperfine field values of the distribution.  $B_{\text{hf}}$  is the hyperfine field with the highest probability.

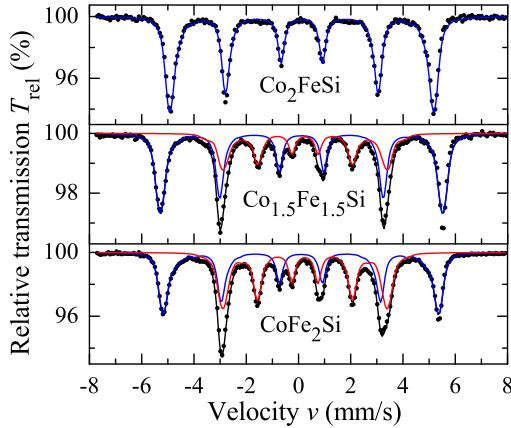


FIG. 5. (Color online) Representative  $^{57}\text{Fe}$  Mössbauer spectra of  $\text{Co}_{1+x}\text{Fe}_{2-x}\text{Si}$  collected at room temperature. Solid lines correspond to the calculated spectra obtained from fits assuming distributions of hyperfine fields. The red and blue lines correspond to the subspectra for the two different iron sites.

The spectrum of  $\text{Co}_2\text{FeSi}$  was fitted by a single hyperfine field distribution (component I). The  $B_{\text{hf}}$  of 31.1 T is in good agreement with Fe atoms located on the  $4a$

position of a regular Heusler structure. Conversely, the spectrum of  $\text{CoFe}_2\text{Si}$  features a second six-line pattern (component II) with a considerably smaller  $B_{\text{hf}}$ . The areas of the subspectra are nearly equal, which verifies that  $\text{CoFe}_2\text{Si}$  adopts a Heusler structure where half of the Co atoms at the  $8c$  sites is replaced by Fe atoms.

Due to the different local environments of the two iron sites, their local magnetic moments  $m_{\text{Fe}}$  and thus their  $B_{\text{hf}}$  values are different. This fact allows unambiguous identification of the two different iron sites. Increasing the iron content in  $\text{Co}_{1+x}\text{Fe}_{2-x}\text{Si}$  leads to a continuous increase of the relative intensity of component II, verifying that the additional Fe atoms successively replace the Co atoms on the  $8c$  positions of the regular structure. The relative area fractions of component II correspond reasonably well to the relative fractions of Fe atoms on the former  $8c$  sites as calculated from the nominal stoichiometry (Table II,  $\text{Fe}(8c)_{\text{area}}$  and  $\text{Fe}(8c)_{\text{calc.}}$ , respectively). These results confirm the high degree of atomic order with respect to occupation of the  $4a$  and former  $8c$  sites by iron. In particular, there is no significant interchange between Fe on the  $4a$  sites and Co, which would lead to a decreased area fraction of component I in the Mössbauer spectra. Therefore, disorder as shown in Figure 6(a) can be excluded.

On the other hand, the  $B_{\text{hf}}$  distributions show a broadening of about 2 – 3 T and some additional asymmetry. As a representative example, the  $B_{\text{hf}}$  distributions for  $x = 1/2$  are shown in Figure 7. All data show a second weak feature for component I with  $B_{\text{hf}}$  being about 3 T smaller than that of the main band, which leads to a slight asymmetry at the lower velocity value side of the peaks of the outer sextet (blue curve in Figure 5). This may indicate a small degree of  $\text{Fe}(4a) - \text{Si}(4b)$  disorder (see Figure 6(b)), which does not change the nearest neighbor environment of iron and thus modifies  $B_{\text{hf}}$  only slightly. The  $B_{\text{hf}}$  distribution of component II is even broader and reveals some asymmetry as well, indicating some Fe – Co disorder on the former  $8c$  positions. This corresponds to disorder of the kind shown in Figure 6(c).

The present spectra confirm the trends in the isomer shifts and hyperfine fields reported previously<sup>16,26</sup>. In



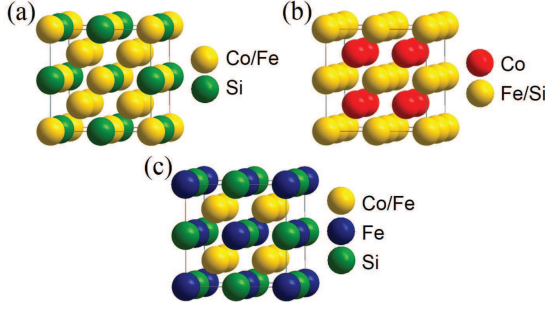


FIG. 6. (Color online) Examples for the possible disorders occurring in the series  $\text{Co}_{1+x}\text{Fe}_{2-x}\text{Si}$  (a)  $\text{D0}_3$ -type disorder between Fe and Co on the 8c and 4a Wyckoff positions; (b)  $\text{B2}$ -type disorder between Fe and Si on the 4a and 4b Wyckoff positions; (c)  $\text{L2}_{1b}$ -type disorder between Co and Fe on the 8c Wyckoff positions.

particular, that both the most probable  $B_{\text{hf}}$  value and the  $IS$  of component I depend slightly on the composition and thus on  $N_v$ . Whereas  $IS$  increases with  $N_v$ , a broad maximum near  $N_v = 29.5$  (Table II) is observed for  $B_{\text{hf}}$ . Remarkably, the trend in  $B_{\text{hf}}$  of component I is similar to the trend in the Curie temperatures (Figure 8 (b), (c)). On the other hand, both,  $IS$  and  $B_{\text{hf}}$  of component II are nearly constant. The small variation of the hyperfine fields within the  $\text{Co}_{1+x}\text{Fe}_{2-x}\text{Si}$  series indicates that the changes in the iron magnetic moments in response to the change in valence electron concentration are small. It is rather the cobalt moment which is altered.

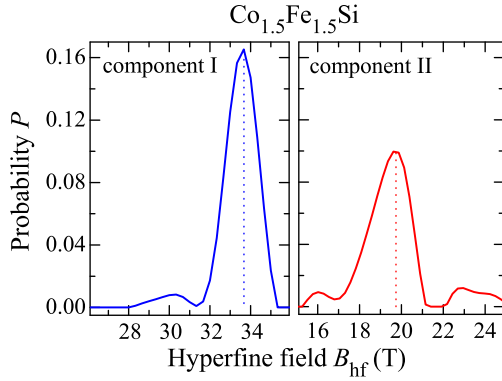


FIG. 7. (Color online) Hyperfine field distributions for components I and II of  $\text{Co}_{1.5}\text{Fe}_{1.5}\text{Si}$  obtained from the data analysis of the corresponding Mössbauer spectrum (Figure 5). The labels I and II correspond to the Fe atoms on the 4a and former 8c sites, respectively. The dotted lines indicate the most probable  $B_{\text{hf}}$  values given in Table II.

The Mössbauer data may be used to estimate the local magnetic moments when it is assumed that the magnetic hyperfine field is proportional to the ordered magnetic moment  $m_{\text{Fe}}$  at the corresponding iron site. Choosing the effective hyperfine coupling constant  $A = 12.5 \text{ T}/\mu_{\text{B}}$  [27] as in previous work on Heusler phases  $\text{Fe}_2\text{YZ}$  [28] and as-

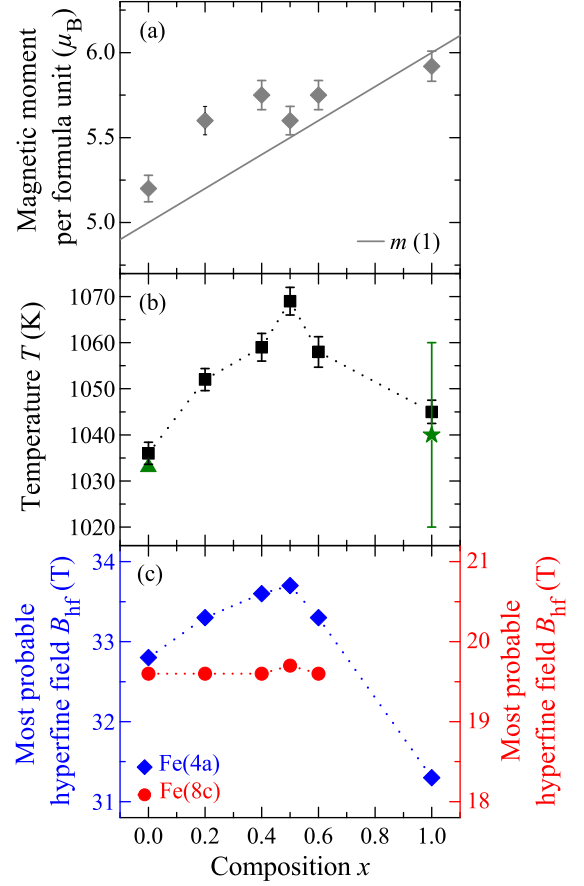


FIG. 8. (Color online) (a) Trend of the magnetic moment per formula unit  $m$  as a function of the composition  $x$ . The solid line corresponds to the moment calculated from equation (1). (b) The Curie temperatures of the  $\text{Co}_{1+x}\text{Fe}_{2-x}\text{Si}$ -series. The star is the value for the inflection point from the magnetic measurement of Reference [10] and the triangle is the value extracted from the inflection point of the curves (with permission) measured by Du *et al.*<sup>14</sup> (no error bars were given). (c) The most probable hyperfine fields of iron on the 4a and former 8c Wyckoff positions of the  $\text{Co}_{1+x}\text{Fe}_{2-x}\text{Si}$ -series as functions of  $x$ . Dotted lines are to guide the eye.

suming that  $A$  does not change within the limited range of compositions considered here, one obtains the magnetic moments on the two iron sites given in Table II. The moments on the 4a sites are about  $1 \mu_{\text{B}}$  larger than those on the former 8c sites.

Additionally, considering the total magnetic moment from the magnetization studies the local magnetic moment ( $m_{\text{Co}}$ ) of the Co atoms can be estimated. This analysis suggests that the increase in the total magnetic moment with increasing valence electron concentration mainly results from an increased local magnetic moment at the Co sites (Table II). The slight variation of the hyperfine fields at the 4a sites then may be attributed to a slight modulation of the magnetic moment by about  $0.2 \mu_{\text{B}}$  within the  $\text{Co}_{1+x}\text{Fe}_{2-x}\text{Si}$  series, whereas the magnetic moments of the iron atoms entering the former 8c

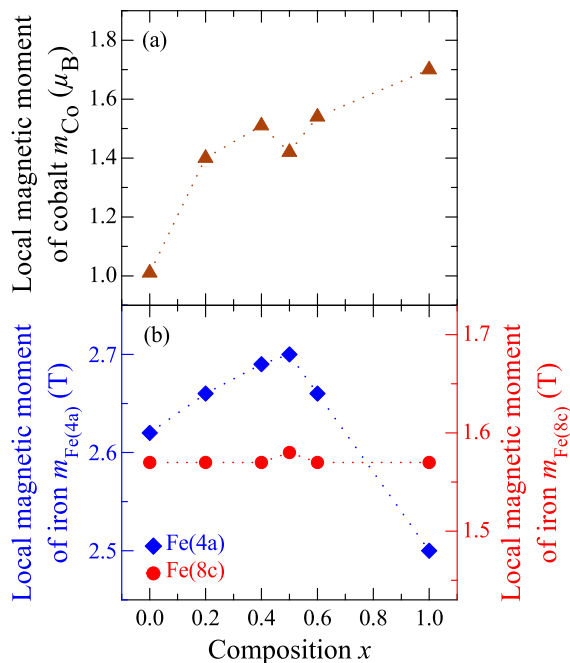


FIG. 9. (Color online) (a) The local magnetic moment of the Co atoms and (b) the local magnetic moments of the different Fe atoms as estimated from  $B_{\text{hf}}$  as functions of  $x$ . Dotted lines are to guide the eye.

sites are essentially independent of  $x$ .

The present analysis yields reasonable estimates for the local moments of  $\text{Co}_2\text{FeSi}$  and  $\text{CoFe}_2\text{Si}$ . The estimated moments of  $2.5 \mu_B$  and  $1.7 \mu_B$  for Fe and Co are in good agreement with the corresponding moments of  $2.4 \mu_B$  and  $1.7 \mu_B$  derived from a neutron diffraction study of  $\text{Co}_2\text{FeSi}$  [29]. In the case of  $\text{CoFe}_2\text{Si}$ , a moment of  $2.6 \mu_B$  for the Fe 4a sites is obtained from both the present Mössbauer analysis and the neutron diffraction data<sup>29</sup>. However, for all alloys containing cobalt as well as iron atoms on the 8c-like sites, the corresponding magnetic moments obtained from neutron diffraction are averages which cannot be decomposed without further assumptions. Niculescu *et al.*<sup>29</sup> assumed that  $m_{\text{Co}}$  is constant ( $= 1.7 \mu_B$ ) within the whole series of  $\text{Fe}_{3-y}\text{Co}_y\text{Si}$  with  $y \leq 2$  (which corresponds to  $-1 \leq x \leq +1$  in our notation  $\text{Co}_{1+x}\text{Fe}_{2-x}\text{Si}$ ). With this assumption the iron magnetic moments at the 8c-like sites were calculated and found to vary with composition. However, electronic structure calculations on  $\text{CoFe}_2\text{Si}$ <sup>30</sup> as well as on the germanium analog  $\text{CoFe}_2\text{Ge}$  [28 and 31] all yield local cobalt moments of about  $1 \mu_B$ , in agreement with our analysis of the Mössbauer data of  $\text{CoFe}_2\text{Si}$  (Table II) and  $\text{CoFe}_2\text{Ge}$  [28]. The electronic structure calculations support the observation that it is mainly the cobalt moment that increases with increasing valence electron concentration.

In a work critically discussing the estimation of magnetic moments from Mössbauer hyperfine fields<sup>32</sup> it was deduced that the effective hyperfine coupling constants

for the two iron sites in  $\text{Fe}_{3-y}\text{Co}_y\text{Si}$  alloys may differ by a factor of up to two in the composition range considered here. As this deduction was based on the analysis of the neutron diffraction data by Niculescu *et al.*<sup>29</sup>, who assumed a unique cobalt moment, the large difference in the  $A$  values between the two sites is possibly an artifact. Although the present estimates of the local moments are in reasonable agreement with experimental and theoretical data, it cannot be excluded that due to polarization contributions to  $B_{\text{hf}}$  from the environment of the Fe sites the  $A$  values are not completely independent from composition. This may modify somewhat the detailed values of the moments and the assignment of the small  $B_{\text{hf}}$  variation of component I to a moment modulation at the Fe 4a sites may not be unambiguous.

#### IV. DISCUSSION

Within the  $\text{Co}_{1+x}\text{Fe}_{2-x}\text{Si}$  series of Heusler compounds ( $0 \leq x \leq 1$ ) the valence electron concentration is changed from 29 for  $\text{Co}_2\text{FeSi}$  to 30 for  $\text{CoFe}_2\text{Si}$ . The Curie temperatures vary between 1036 and 1069 K. The highest  $T_C$  is obtained for the composition  $\text{Co}_{1.5}\text{Fe}_{1.5}\text{Si}$ . The dependence on the composition can be explained by examination of the atomic environments. It was found in earlier work<sup>12</sup> that the  $T_C$  of Co-containing Heusler compounds with different magnetic sublattices depends on the corresponding sublattice transition temperatures. These sublattice transition temperatures are proportional to the spin moments  $S$  and the Heisenberg exchange integral  $J$  between the different sites. These variables are clearly modified with the change in composition and thus the local environments.

As suggested by the analysis of the Mössbauer data, the increase in the total magnetic moment with increasing  $N_v$  is mainly reflected in an increase in the local moment of the cobalt atoms.  $B_{\text{hf}}$  and  $m_{\text{Fe}}$  remain constant for Fe on former 8c sites since their nearest neighbor environment (eight Fe atoms on the 4a positions) remains unchanged. On the contrary, it is noteworthy that  $T_C$  shows a comparable non-monotonic variation as the hyperfine field for the Fe 4a sites (Figure 8). This  $B_{\text{hf}}$  variation is associated with the variation in the local environment of the Fe atoms located on the 4a positions. Their nearest neighbor (NN) Co atoms are consecutively substituted by Fe atoms which introduces disorder. The variation in  $B_{\text{hf}}$  may reflect a variation in the local magnetic moments of iron located on 4a sites. In that case, exchange interactions involving these sites are modified as well.

For the  $\text{Co}_{1+x}\text{Fe}_{2-x}\text{Si}$  series, different exchange coupling integrals need to be considered:  $J_{\text{Co-Co}}$ ,  $J_{\text{Fe-Fe}}$  and  $J_{\text{Co-Fe}}$ . In perfectly ordered regular Heusler type  $\text{Co}_2\text{FeSi}$ ,  $J_{\text{Fe}(4a)-\text{Co}(8c)}$  (NN) and  $J_{\text{Co}(8c)-\text{Co}(8c)}$  (next nearest neighbors, NNN) occur. There are no Fe-Fe interactions present. In the ordered inverse Heusler structure of  $\text{CoFe}_2\text{Si}$ ,  $J_{\text{Fe}(4a)-\text{Co}(4c)}$  and  $J_{\text{Fe}(4a)-\text{Fe}(4d)}$  are

TABLE II. Results from the magnetic measurements and  $^{57}\text{Fe}$  Mössbauer spectroscopy on  $\text{Co}_{1+x}\text{Fe}_{2-x}\text{Si}$  related to the composition  $x$  and the number of valence electrons  $N_v$ . The values for the average hyperfine fields of the distributions  $\langle B_{\text{hf}} \rangle$  and for the hyperfine fields with the most probable  $B_{\text{hf}}$  are given in Tesla and have an error of  $\pm 0.1$  T. The isomer shift  $IS$  is given in mm/s with an uncertainty of  $\pm 0.001$  mm/s. For labelling the two different iron sites we use the Wyckoff positions of the  $x = 1$  compound  $\text{Co}_2\text{FeSi}$  though due to replacement of Co by Fe the actual symmetry is lowered.  $\text{Fe}(8c)_{\text{area}}$  corresponds to the Fe fraction at the former 8c sites obtained from the Mössbauer spectra.  $\text{Fe}(8c)_{\text{calc.}}$  is the corresponding Fe fraction calculated from stoichiometry. The magnetic moment per formula unit  $m$  has a standard deviation of 1.5%. The relative error of the determined Curie temperature is 0.4%.

$x$	$N_v$	Fe(4a)			Fe(8c)			$\text{Fe}(8c)_{\text{area}}$ (%)	$\text{Fe}(8c)_{\text{calc.}}$ (%)	$m_{\text{Fe}(4a)}$ ( $\mu_B$ )	$m_{\text{Fe}(8c)}$ ( $\mu_B$ )	$m$ ( $\mu_B$ )	$m_{\text{Co}}$ ( $\mu_B$ )	$T_C$ (K)
		$IS$	$\langle B_{\text{hf}} \rangle$	$B_{\text{hf}}$	$IS$	$\langle B_{\text{hf}} \rangle$	$B_{\text{hf}}$							
0	29.0	0.093	32.2	32.8	0.250	19.5	19.6	49.1	50.0	2.62	1.57	5.20	1.01	1036
0.2	29.2	0.099	32.9	33.3	0.250	19.4	19.6	44.3	44.4	2.66	1.57	5.60	1.40	1052
0.4	29.4	0.109	33.0	33.6	0.252	19.4	19.6	38.5	37.0	2.69	1.57	5.75	1.51	1059
0.5	29.5	0.113	33.4	33.7	0.252	19.6	19.7	34.6	33.3	2.70	1.58	5.62	1.42	1069
0.6	29.6	0.118	33.0	33.3	0.245	19.3	19.6	31.0	28.5	2.66	1.57	5.75	1.54	1058
1	30.0	0.125	31.1	31.3	-	-	-	0	0	2.50	-	5.92	1.71	1045

present in the NN shells and  $J_{\text{Fe}(4d)-\text{Co}(4c)}$  occurs between NNN. No Co-Co interactions arise in the first two atomic shells. In the off-stoichiometric compounds, all combinations of Heisenberg exchange integrals are present. Additionally, in the disordered structures with  $x \neq 1$ , Fe atoms located on the former 8c positions may couple with Fe atoms on equal crystallographic sites. Thus, only in the disordered samples additional  $J_{\text{Fe}(8c)-\text{Fe}(8c)}$  occurs between NNN. It seems likely that this additional Heisenberg exchange integral plays an important role on the  $T_C$  in the off-stoichiometric samples.

The effect of disorder on  $T_C$  in this system is surprising. Generally, disorder tends to reduce  $T_C$ , with the most extreme case being amorphous transition metal alloys, which lack short and long range chemical and structural order. These exhibit a reduced Curie temperature in comparison to their crystalline analog<sup>33</sup>. Remarkably, in this system changes in the site occupancy actually increase  $T_C$ . The modulation of the exchange energies due to variations in magnetic moments and exchange integrals are the likely origin for this behavior.

## V. CONCLUSION

A series of Heusler compounds of the composition  $\text{Co}_{1+x}\text{Fe}_{2-x}\text{Si}$  ( $0 \leq x \leq 1$ ) with high Curie temperatures was synthesized to study trends in  $m$  and  $T_C$  in a small range of valence electron concentrations.  $^{57}\text{Fe}$  Mössbauer spectroscopy confirmed that in the off-stoichiometric compounds the additional Fe atoms replace the Co atoms at the 8c positions successively causing L2<sub>1b</sub>-type disorder.

der.

The total magnetic moment  $m$  increases with increasing  $N_v$  comparable to variations in the local magnetic moment of cobalt derived from the Mössbauer data. A maximum Curie temperature of 1069 K is observed for the composition with  $x = 0.5$ . The hyperfine fields corresponding to iron on the 4a sites follow a trend comparable to that of the  $T_C$ , which may reflect a similar variation in the local magnetic moments of Fe atoms located on these positions. The  $B_{\text{hf}}$  of iron atoms located on the former 8c positions is constant with composition reflecting a well-ordered nearest neighbor environment (Fe(4a)-Si(4b)).

In addition, the variations in the site occupancy and changes in the local atomic environments modify the corresponding Heisenberg exchange integrals. Both factors, local magnetic moments and exchange integrals, must be examined carefully to understand the trend in the  $T_C$ . Theoretical analysis is highly desirable for an in-depth understanding of this behavior.

## ACKNOWLEDGMENTS

The authors gratefully acknowledge Lukas Wollmann for helpful discussions, Walter Schnelle for performing magnetic measurements, Silvia Kostmann and Monika Eckert for the microstructural analysis, Horst Borrmann for the X-Ray diffraction measurements and Ulrike Schmidt and Anja Völzke for chemical analysis. This work was financially supported by the ERC Advanced Grant no. 291472 *Idea Heusler*.

\* julie.karel@cpfs.mpg.de

<sup>1</sup> C. Felser, G. H. Fecher, and B. Balke,

Angew. Chem. Int. Ed. **46**, 668 (2007).

<sup>2</sup> M. Kawano, M. Ikawa, K. Arima, T. Kanashima, and

- K. Hamaya, J. Appl. Phys. **119**, 045302 (2016).
- <sup>3</sup> Y. Kasatan, S. Yamada, H. Itoh, M. Miyao, K. Hamaya, and Y. Noozaki, Appl. Phys. Express **7**, 123001 (2014).
  - <sup>4</sup> B. K. Hazra, M. M. Raja, and S. Srinath, J. Phys. D: Appl. Phys. **49**, 065007 (2016).
  - <sup>5</sup> B. Balke, S. Wurmehl, G. H. Fecher, C. Felser, and J. Kübler, Sci. Tech. Adv. Mater. **9**, 014102 (2008).
  - <sup>6</sup> S. Wurmehl, G. H. Fecher, K. Kroth, F. Kronast, H. A. Dürr, Y. Takeda, Y. Saitoh, K. Kobayashi, H. Lin, G. Schönhense, and C. Felser, J. Phys. D: Appl. Phys. **39**, 803 (2006).
  - <sup>7</sup> K. Inomata, S. Okamura, A. Miyazaki, M. Kikuchi, N. Tezuka, M. Wojcik, and E. Jedryka, J. Phys. D: Appl. Phys. **39**, 816 (2006).
  - <sup>8</sup> I. Galanakis, P. Dederichs, and N. Papanikolaou, Phys. Rev. B **66**, 174429 (2002).
  - <sup>9</sup> M. Jourdan, A. Kronenberg, M. Kolbe, H. Elmers, G. Schönhense, M. Klau, J. Minar, J. Braun, H. Ebert, and S. Chadov, Nat. Commun. **5**, 3947 (2014).
  - <sup>10</sup> S. Wurmehl, G. H. Fecher, V. Ksenofontov, F. Casper, U. Stumm, C. Felser, H. Lin, and Y. Hwu, J. Appl. Phys. **99**, 08J103 (2006).
  - <sup>11</sup> J. Kübler, *Theory of Itinerant Electron Magnetism* (Oxford University Press, Oxford, 2009).
  - <sup>12</sup> G. H. Fecher, H. C. Kandpal, S. Wurmehl, C. Felser, and G. Schönhense, J. Appl. Phys. **99**, 08J106 (2006).
  - <sup>13</sup> J. Kübler, G. H. Fecher, and C. Felser, Phys. Rev. B **76**, 024414 (2007).
  - <sup>14</sup> Y. Du, G. Z. Xu, X. M. Zhang, Z. Y. Liu, S. Y. Yu, E. K. Liu, W. H. Wang, and G. H. Wu, Europhys. Lett. **103**, 37011 (2013).
  - <sup>15</sup> K. H. J. Buschow, P. G. V. Engen, and R. Jongebreur, J. Magn. Magn. Mater. **38**, 1 (1983).
  - <sup>16</sup> V. Jung, B. Balke, G. H. Fecher, and C. Felser, Appl. Phys. Lett. **93**, 042507 (2008).
  - <sup>17</sup> H. Luo, Z. Zhu, L. Ma, S. Xu, H. Liu, J. Qu, Y. Li, and G. Wu, J. Phys. D: Appl. Phys. **40**, 7121 (2007).
  - <sup>18</sup> STOE WinXPOW Version 2.25, Stoe & Cie GmbH, Darmstadt, Germany, 2009.
  - <sup>19</sup> PowderCell for Windows Version 2.4, Federal Institute for Materials Research and Testing, Berlin, Germany, 2009.
  - <sup>20</sup> Website: <http://www.mosswinn.com/>.
  - <sup>21</sup> R. Grössinger, G. Hilscher, and H. Kirchmayr, Mikrochim. Acta **9**, 161 (1981).
  - <sup>22</sup> S. Wurmehl, G. H. Fecher, H. C. Kandpal, V. Ksenofontov, C. Felser, and H. Lin, Appl. Phys. Lett. **88**, 032503 (2006).
  - <sup>23</sup> V. Niculescu, T. J. Burch, K. Raj, and J. I. Budnick, J. Magn. Magn. Mater. **5**, 60 (1977).
  - <sup>24</sup> N. N. Greenwood and A. Earnshaw, *Chemistry of the Elements* (Butterworth-Heinemann, Oxford, 2002).
  - <sup>25</sup> S. Wurmehl, G. Fecher, H. Kandpal, V. Ksenofontov, C. Felser, H. Lin, and J. Morais, Phys. Rev. B **72**, 184434 (2005).
  - <sup>26</sup> V. Ksenofontov, M. Wójcik, S. Wurmehl, H. Schneider, B. Balke, G. Jakob, and C. Felser, J. Appl. Phys. **107**, 09B106 (2010).
  - <sup>27</sup> O. Massenet, H. Daver, V. D. Nguyen, and J. P. Rebouillat, J. Phys. F: Met. Phys. **9**, 1678 (1979).
  - <sup>28</sup> T. Gasi, V. Ksenofontov, J. Kiss, S. Chadov, A. Nayak, M. Nicklas, J. Winterlik, M. Schwall, P. Klaer, P. Adler, and C. Felser, Phys. Rev. B **87**, 064411 (2013).
  - <sup>29</sup> V. Niculescu, J. I. Budnick, W. A. Hines, K. Raj, S. Pickart, and S. Skalski, Phys. Rev. B **19**, 452 (1979).
  - <sup>30</sup> H. Luo, F. Meng, Y. Cai, W. Hong, E. Liu, G. Wu, X. Zhu, and C. Jiang, J. Magn. Magn. Mater. **323**, 2323 (2011).
  - <sup>31</sup> Z. Ren, S. T. Li, and H. Z. Lu, Physica B **405**, 2840 (2010).
  - <sup>32</sup> S. M. Dubiel, J. Alloys Compd. **488**, 18 (2009).
  - <sup>33</sup> K. Moorjani and J. M. D. Coey, *Magnetic Glasses* (Elsevier, New York, 1984).